Nuclear Engineering and Technology 49 (2017) 1125–1134

Contents lists available at ScienceDirect

Nuclear Engineering and Technology

journal homepage: www.elsevier.com/locate/net

Original Article

A multilevel in space and energy solver for multigroup diffusion eigenvalue problems

Ben C. Yee*, Brendan Kochunas, Edward W. Larsen

Department of Nuclear Engineering and Radiological Sciences, University of Michigan, Ann Arbor, MI 48109, USA

ARTICLE INFO

Article history:
Received 2 June 2017
Received in revised form
14 July 2017
Accepted 27 July 2017
Available online 5 August 2017

Keywords:
Multigroup diffusion
Multilevel
Eigenvalue

ABSTRACT

In this paper, we present a new multilevel in space and energy diffusion (MSED) method for solving multigroup diffusion eigenvalue problems. The MSED method can be described as a PI scheme with three additional features: (1) a grey (one-group) diffusion equation used to efficiently converge the fission source and eigenvalue, (2) a space-dependent Wielandt shift technique used to reduce the number of PIs required, and (3) a multigrid-in-space linear solver for the linear solves required by each PI step. In MSED, the convergence of the solution of the multigroup diffusion eigenvalue problem is accelerated by performing work on lower-order equations with only one group and/or coarser spatial grids. Results from several Fourier analyses and a one-dimensional test code are provided to verify the efficiency of the MSED method and to justify the incorporation of the grey diffusion equation and the multigrid linear solver. These results highlight the potential efficiency of the MSED method as a solver for multidimensional multigroup diffusion eigenvalue problems, and they serve as a proof of principle for future work. Our ultimate goal is to implement the MSED method as an efficient solver for the two-dimensional/three-dimensional coarse mesh finite difference diffusion system in the Michigan parallel characteristics transport code. The work in this paper represents a necessary step towards that goal.

1. Introduction

The multigroup diffusion eigenvalue problem is an approximation to the multigroup neutron transport eigenvalue problem that is widely used for reactor physics simulations. The solution is frequently used to accelerate the source iteration procedure for solving neutron transport problems via methods such as coarse mesh finite difference (CMFD) [1]. Although solving a diffusion problem requires significantly fewer computational resources than solving a transport problem, this cost is still not trivial. Many transport codes that use CMFD-like procedures (e.g., the Michigan parallel characteristics transport (MPACT) code [2]) have a CMFD eigenvalue problem with hundreds of millions of unknowns, and obtaining solutions to this problem constitutes a large portion of the computational effort.

In this work, we introduce a new multilevel in space and energy diffusion (MSED) method for solving the multigroup diffusion eigenvalue problem. This is a multicomponent method that draws from existing ideas (multigrid-in-space [3] and two-grid in energy [4]) as well as new ideas (space-dependent Wielandt shift [5]). The three primary components of MSED are: (1) a “grey” (one-group) diffusion equation, used to converge the eigenvalue and fission source, (2) a space-dependent Wielandt shift, used to reduce the number of power iterations (PIs) required for convergence, and (3) a multigrid-in-space solver, used to solve the fixed-source grey and multigroup diffusion linear systems.

The MSED method can be viewed as an extension of the CMFD method. In CMFD, the convergence of a higher-order (more unknowns) transport or nodal diffusion system is accelerated by leveraging a lower-order diffusion system. In MSED, this lower-order diffusion system is itself accelerated by simpler diffusion equations with even fewer unknowns. Fig. 1A provides a visualization of this hierarchy. Alternatively, the MSED method can be viewed as an extension of the multigrid method to nonspatial variables. Fig. 1B provides a visualization of the changes in spatial and energy grid sizes in the MSED iteration scheme. These two figures are further explained in Sections 2 and 3.

Of the methods that have been developed for reactor physics simulations, the multilevel coarse mesh rebalance (MLCMR) and multilevel surface rebalance (MLSR) methods developed by van

* Corresponding author.
E-mail addresses: bcyee@umich.edu (B.C. Yee), bkochuna@umich.edu (B. Kochunas), edlarsen@umich.edu (E.W. Larsen).

http://dx.doi.org/10.1016/j.net.2017.07.014

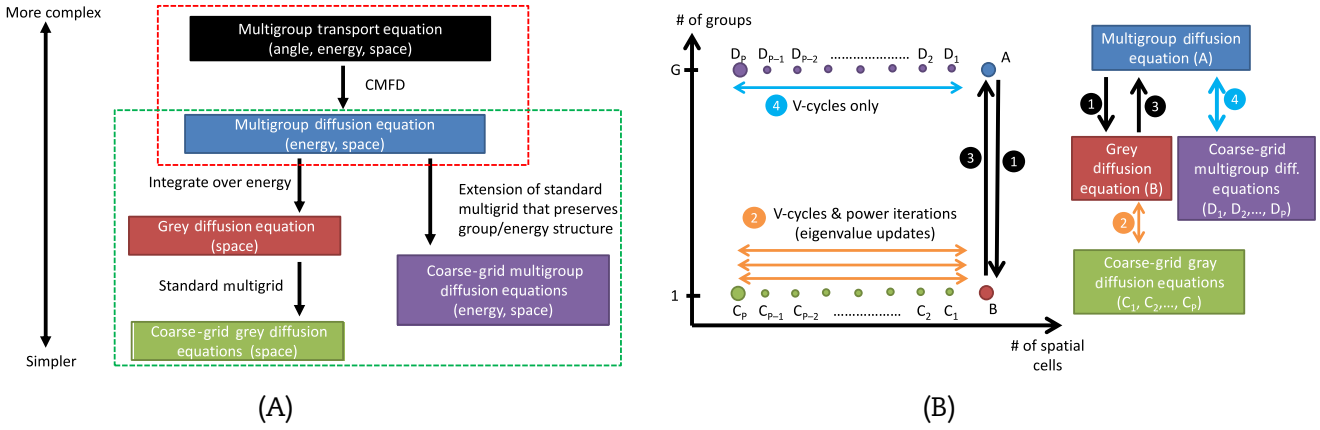

Fig. 1. Each figure provides an overview of the MSED iteration procedure. (A) The hierarchy of the equations in MSED is shown, with a scale on the left describing the relative complexity of these equations (i.e., the number of unknowns). The higher (red) dashed box encloses the equations used in the CMFD method, while the lower (green) dashed box encloses the equations used in the MSED method. (B) An MSED iteration is broken up into four steps, and the changes in the energy and spatial grid sizes at each step are visualized.

Geemert and others [6–8] are the most similar to MSED. The MLCMR and MLSR methods are techniques for nodal diffusion problems, which leverage solutions from a series of lower-order coarse-grid one-group diffusion equations in order to minimize the number of iterations required on the full higher-order nodal diffusion equations. In this sense, the approaches taken by the MSED method and the MLCMR/MLSR methods are similar—both methods minimize the computational effort required by shifting iterations from higher-order equations to lower-order equations that are less costly to solve. The MSED method is also similar to multilevel CMFD methods [1,9,10]. In these cited works, the multigroup CMFD equations are themselves accelerated by two-group CMFD equations.

The MSED method draws from elements of both the rebalance and multilevel CMFD concepts, but there are several important distinctions. First, the CMFD problem motivating the development of MSED is orders of magnitude larger (in terms of the number of unknowns and the number of processors used) than any of the applications in the works referenced above. Second, unlike the MLCMR/MLSR techniques, MSED operates on a diffusion/CMFD system in which the unknowns representing the neutron net current have already been eliminated—this simplifies the process of collapsing onto coarser spatial/energy grids. Third, whereas the multilevel CMFD techniques use flux-weighted cross-sections and low-order "consistency factors" (commonly denoted by $\hat{D}$, and sometimes described as a "drift" vector/term) to generate its group-collapsed equations, the MSED method uses both flux-weighted cross-sections *and* flux-weighted diffusion coefficients, and does not need additional "consistency factors" like the $\hat{D}$ in the multilevel CMFD methods. In this sense, the collapse in energy in MSED is similar to that of the MLCMR/MLSR methods. Another example in which the diffusion coefficients are group-collapsed via flux-weighting can be found in Schunert et al. [11]; there, the S_N FEM-discretized transport equations are accelerated by coarse-group FEM-discretized diffusion equations. However, the coarsening in space in MSED differs from all of the aforementioned examples—the spatial variable in MSED is collapsed using a standard multigrid approach in which coarse-grid equations are error equations rather than approximations to the original system. Moreover, this collapse in MSED is performed on both the grey *and* the multigroup equations, as illustrated by Fig. 1B.

Lastly, we note that, like the MLCMR/MLSR methods, MSED uses a one-group (grey) low-order equation rather than a two-group equation. Although the referenced multilevel CMFD methods all use a two-group structure as their coarsest energy grid, we have found that the MSED method with a grey equation already performs very well. Our Fourier analysis and numerical results indicate that the MSED method, as described in this paper, has a spectral radius of ~0.1. Because of this low spectral radius and the fact that a grey system is simpler (easier to implement and solve) than a two-group system, we have not yet been compelled to study the use of a two-group system in the MSED method. Recent work by Cornejo and Anistratov, however, has shown that additional energy grid(s) between one group and G groups [12,13] can provide tangible improvements in the runtime, and it may be possible to use a similar strategy to improve the MSED algorithm. In future work, we will assess the potential benefit of both introducing an extra two-group system to MSED and replacing the one-group system in MSED with a two-group system.

Another motivation for the development of the MSED method is to reduce the reliance of MPACT on "black-box" Krylov linear solvers. In recent years, many diffusion and CMFD codes have become increasingly reliant on Krylov methods for solving their linear systems. These methods are generally easy to implement due to their availability in various linear algebra libraries such as PETSc [14]. They perform reasonably well when compared to other frequently used linear solvers such as SOR or Gauss–Seidel. However, many Krylov solvers (GMRES in particular) require a significant amount of memory and may not be well-suited for high-performance computing applications where memory is a limiting resource. Moreover, Krylov methods generally do not account for the physics and structure of the problem being solved, and their convergence is typically slow for large problems unless a good physics-based or problem-dependent preconditioner is applied to the system. In many cases, such a preconditioner may not be known and, even if one exists, constructing the preconditioner and applying it to the linear system may require a significant computational effort. The approach taken by MSED is fundamentally different from those taken by the Krylov methods. Whereas Krylov methods are applicable to general linear systems, MSED is optimized only for multigroup diffusion/CMFD eigenvalue problems. MSED leverages our knowledge of the physics and structure of the multigroup diffusion problem and is designed to exploit the unique features of this problem.

In the following sections, we provide an overview of the theory for the three components of MSED, describe the full algorithm, and present results from our Fourier analysis and one-dimensional (1D) test code. This paper should be viewed as an initial report for the development of the MSED method, and the work presented in this paper is a necessary initial step towards our ultimate goal of

implementing MSED as a solver for the multidimensional CMFD problem in MPACT. As this development progresses and as we learn more about the performance of the MSED method, it is likely that changes will be made to the algorithm so that it performs optimally in parallel on both two-dimensional (2D) and three-dimensional (3D) CMFD problems.

2. Theory

The 1D multigroup diffusion equation (the blue box in Fig. 1A), discretized using a second-order finite-difference scheme, is given by:

$$-\frac{1}{\Delta x_j}\left[D_{j+\frac{1}{2},g}\frac{\phi_{j+1,g}-\phi_{j,g}}{\Delta x_{j+\frac{1}{2}}}-D_{j-\frac{1}{2},g}\frac{\phi_{j,g}-\phi_{j-1,g}}{\Delta x_{j-\frac{1}{2}}}\right]+\Sigma_{t,j,g}\phi_{j,g}-\sum_{g'=1}^{G}\Sigma_{s0,j,g'\to g}\phi_{j,g'}=\lambda\chi_{j,g}\sum_{g'=1}^{G}\nu\Sigma_{f,j,g'}\phi_{j,g'} \tag{1}$$

Here, j is the spatial index, g is the group index, G is the number of groups, $D_{j+½,g}$ is the diffusion coefficient, $\Sigma_{t,j,g}$ is the total cross-section, $\Sigma'_{s0,j,g\to g}$ is the differential scattering cross-section, $\nu\Sigma_{f,j,g}$ is the neutron multiplicity times the fission cross-section, $\chi_{j,g}$ is the fission spectrum, $\phi_{j,g}$ is the multigroup scalar flux (spatially averaged over cell j), Δx_j is the width of cell j, and

$$\Delta x_{j+\frac{1}{2}}\equiv\frac{1}{2}\left[\Delta x_j+\Delta x_{j+1}\right]. \tag{2}$$

Eq. (1) is often represented using matrix or operator notation as

$$\underline{\underline{M}}\,\underline{\phi}=\lambda\underline{\underline{F}}\,\underline{\phi}. \tag{3}$$

In this paper, a double underscore denotes a matrix while a single underscore denotes a column vector.

Although a CMFD system differs slightly from Eq. (1) due to the presence of correction factors from the transport system, we can account for these correction factors with a minor modification—this is discussed briefly in Section 2.2. The remainder of the theory presented in this paper can be applied to both diffusion and CMFD systems with no other modifications.

For simplicity and brevity, we only present the theory for the MSED method in one dimension for the specific finite-difference spatial discretization in Eq. (1). This spatial discretization is used by most CMFD systems, including the one in MPACT. The generalization of the theory to two and three dimensions is straightforward; we would only need to add spatial indices to the subscripts and additional leakage terms. Moreover, the geometric multigrid method described in Section 2.2 is still valid in higher dimensions, provided that the spatial grid is Cartesian. The generalization of the MSED method to other spatial discretizations is less straightforward but should be possible if one carefully modifies the definitions of the grey diffusion coefficients (Eq. (6d)) and the spatial interpolation and restriction operators of the multigrid solver (Eqs. (15)).

The remainder of this section consists of four subsections, each describing one algorithm that is a component of the MSED method. The first subsection describes the standard PI method for solving Eq. (1). Subsequent subsections describe how each component of MSED is used to improve standard PI.

2.1. Power iteration

The standard PI scheme for solving diffusion eigenvalue problems can be defined as follows:

$$-\frac{1}{\Delta x_j}\left[D_{j+\frac{1}{2},g}\frac{\phi^{(l+\frac{1}{2})}_{j+1,g}-\phi^{(l+\frac{1}{2})}_{j,g}}{\Delta x_{j+\frac{1}{2}}}-D_{j-\frac{1}{2},g}\frac{\phi^{(l+\frac{1}{2})}_{j,g}-\phi^{(l+\frac{1}{2})}_{j-1,g}}{\Delta x_{j-\frac{1}{2}}}\right]+\Sigma_{t,j,g}\phi^{(l+\frac{1}{2})}_{j,g}-\sum_{g'=1}^{G}\Sigma_{s0,j,g'\to g}\phi^{(l+\frac{1}{2})}_{j,g'}=\lambda^{(l)}\chi_{j,g}\sum_{g'=1}^{G}\nu\Sigma_{f,j,g'}\phi^{(l)}_{j,g'}, \tag{4a}$$

$$\lambda^{(l+1)}=\lambda^{(l)}\frac{\sum_{g'=1}^{G}\sum_j\nu\Sigma_{f,j,g'}\phi^{(l)}_{j,g'}}{\sum_{g'=1}^{G}\sum_j\nu\Sigma_{f,g'}\phi^{(l+\frac{1}{2})}_{j,g'}}, \tag{4b}$$

$$\phi^{(l+1)}_{j,g}=\left\|\underline{\phi}^{(l+\frac{1}{2})}\right\|^{-1}\phi^{(l+\frac{1}{2})}_{j,g}. \tag{4c}$$

Here, l is the iteration index for PI.

Algorithm 1: A standard PI step

Input: $\phi^{(l)}_{j,g}$, $\lambda^{(l)}$

Result: $\phi^{(l+1)}_{j,g}$, $\lambda^{(l+1)}$

1. Update the scalar flux using Eq. (4a).
2. Update the eigenvalue using Eq. (4b).
3. Renormalize the scalar flux using Eq. (4c).

In the following subsections, three modifications are made to Algorithm 1 in order to establish the MSED method illustrated in Fig. 1. Each subsection describes a modification, the motivation for that modification, and its effect on accelerating the PI scheme. In Section 3, we combine these components (Algorithms 2-4) to create Algorithm 5, which describes the full MSED iteration scheme depicted in Fig. 1.

2.2. Grey diffusion equation

The first and perhaps most important component of the MSED method is the grey (one-group) diffusion equation (the box with the solid red background in Fig. 1A). We note that the term "grey" is not typically used in reactor physics. The history of this term stems from the study of the radiative transfer equations, and in particular, this term is frequently used when describing the numerical simulation of these equations for astrophysics and atmospheric applications. Despite its origins, we feel that it is appropriate to use the term "grey" in this paper, as the development of our grey diffusion equation was strongly motivated by our knowledge of similar concepts in radiative transfer. When numerically simulating radiative transfer, a grey diffusion or transport equation is often used to accelerate the convergence of the more complex, multifrequency (i.e., energy-dependent or multigroup) radiative transfer problems through some scale-bridging Algorithm [15,16]. In our work, the purpose of the grey diffusion equation is more or less the same; we use the grey diffusion system to accelerate the convergence of the more complex multigroup diffusion system.

To derive the grey diffusion equation, we sum Eq. (1) over the groups g. The collapse is straightforward for all of the terms except the leakage term. Performing the collapse yields the following grey equation:

$$-\left[\frac{\left\langle D_{j+\frac{1}{2}j+1}\right\rangle}{\Delta x_j \Delta x_{j+\frac{1}{2}}}\right]\Phi_{j+1}-\left[\frac{\left\langle D_{j-\frac{1}{2}j-1}\right\rangle}{\Delta x_j \Delta x_{j-\frac{1}{2}}}\right]\Phi_{j-1}+\left[\frac{\left\langle D_{j+\frac{1}{2}j}\right\rangle}{\Delta x_j \Delta x_{j+\frac{1}{2}}}+\frac{\left\langle D_{j-\frac{1}{2}j}\right\rangle}{\Delta x_j \Delta x_{j-\frac{1}{2}}}+\left\langle \Sigma_{a,j}\right\rangle\right]\Phi_j=\lambda\left\langle \nu\Sigma_{f,j}\right\rangle\Phi_j. \tag{5}$$

In this equation, the grey scalar flux and the bracketed grey quantities are given by:

$$\Phi_j \equiv \sum_{g=1}^{G}\phi_{j,g}, \tag{6a}$$

$$\langle \Sigma_{a,j}\rangle \equiv \frac{1}{\Phi_j}\sum_{g=1}^{G}\Sigma_{a,j,g}\phi_{j,g}, \tag{6b}$$

$$\langle \nu\Sigma_{f,j}\rangle \equiv \frac{1}{\Phi_j}\sum_{g=1}^{G}\nu\Sigma_{f,j,g}\phi_{j,g}, \tag{6c}$$

$$\langle D_{j_1,j_2}\rangle \equiv \frac{1}{\Phi_{j_2}}\sum_{g=1}^{G}D_{j_1,g}\phi_{j_2,g}. \tag{6d}$$

Here, $\Sigma_{a,j,g}$ is the absorption cross-section, defined by

$$\Sigma_{a,j,g}=\Sigma_{t,j,g}-\sum_{g'=1}^{G}\Sigma_{s0,j,g\to g'}. \tag{7}$$

The careful collapse of the diffusion coefficient via Eq. (6d) is necessary to ensure that the grey diffusion coefficients are positive and well-defined when $(\Phi_{j+1}-\Phi_j)\to 0$. If a different spatial discretization is used, the collapse of the diffusion coefficients may require modification to ensure consistency and positivity. To account for CMFD correction factors ($\hat{D}$), a minor change can be made to the definition of the collapsed diffusion coefficient in Eq. (6d).

Algorithm 2 briefly describes how the grey diffusion equation can be incorporated into the standard PI scheme. By using a grey equation, Algorithm 2 is able to efficiently converge the eigenvalue and fission source. The basic reason for this efficiency is that the right side of Eq. (1) is separable in the indices g and g'—a mathematical representation of the assumption that the energy of a neutron born from fission is independent of the energy of the incoming neutron that induced the fission. Because of this property, the fission source in a multigroup diffusion eigenvalue problem ($\sum_{g'=1}^{G}\nu\Sigma_{f,j,g'}\phi_{j,g'}$) is naturally a grey quantity. This term is the same for both the grey and multigroup systems upon convergence.

Algorithm 2: A PI step accelerated by a grey diffusion equation.

Input: $\phi_{j,g}^{(l)}$, $\lambda^{(l)}$

Result: $\phi_{j,g}^{(l+1)}$, $\lambda^{(l+1)}$

1. Compute $\Phi^{(l,0)}$ and the grey cross-sections from $\phi_{j,g}^{(l)}$ using Eqs. (6).
2. Perform M PIs (Algorithm 1 with G=1) on the grey diffusion eigenvalue problem (Eq. (5)) to obtain the normalized grey scalar flux $\Phi^{(l,M)}$ and its corresponding eigenvalue $\lambda^{(l,M)}$.

M can be either a fixed number or the number of PIs required to converge the grey diffusion solution to a certain tolerance.

3. Update the multigroup scalar flux and eigenvalue:

$$\phi_{j,g}^{\left(l+\frac{1}{2}\right)}=\phi_{j,g}^{(l)}\frac{\Phi_j^{(l,M)}}{\Phi_j^{(l,0)}}, \tag{8a}$$

$$\lambda^{(l+1)}=\lambda^{(l,M)} \tag{8b}$$

4. Consider Eq. (4a), except with $\lambda^{(l+1)}$ instead of $\lambda^{(l)}$ and with all of the iteration indices on ϕ incremented by 1/2. Solve this equation to obtain $\phi_{j,g}^{(l+1)}$.

Algorithm 2 can still be viewed as a PI scheme on the multigroup system, but it has one important modification: at the beginning of each multigroup PI, we create a grey eigenvalue problem (Step 1), solve the grey eigenvalue problem (Step 2), and use the resulting grey solution to improve the working estimate of the eigenvalue, eigenvector, and fission source (Step 3). Then, in Step 4, a standard PI step is performed on the multigroup diffusion system. Step 4 is a PI in the sense that we are solving a fixed-source problem, in which the source is determined by the current estimate of the eigenvector, in order to obtain an improved estimate of the eigenvector. Because we normalize the eigenvector and update the eigenvalue in the grey system, these steps are not necessary on the multigroup system and are not explicitly included in Algorithm 2. (Nonetheless, we have found that performing an additional update of the eigenvalue after Step 4 of Algorithm 2 can provide a marginal improvement in the convergence of the eigenvalue.)

With the grey diffusion equation providing an efficient means of converging the fission source and eigenvalue, iterations on the multigroup system (Step 4 in Algorithm 2) are only needed to converge the energy dependence of the scalar flux (and, consequently, the scattering source). As a result, the required number of multigroup PIs is one to two orders of magnitude smaller than that of standard PI. Although Algorithm 2 requires PIs on the grey diffusion system in addition to PIs on the multigroup diffusion system, these new grey iterations are significantly cheaper than iterations on the larger multigroup system. In short, the incorporation of the grey diffusion system makes it possible to shift the bulk of the work in the iteration scheme from the multigroup diffusion system to the smaller grey system.

In our work, we have also explored the use of an alternate grey diffusion equation, derived from multiplying Eq. (1) by a space- and group-dependent function $f_{j,g}$ and then summing over g. (In Eq. (5), $f_{j,g}=1$.) A Fourier analysis of this alternate grey diffusion equation indicates that choosing $f_{j,g}$ to be an estimate of the multigroup adjoint eigenfunction leads to an iteration scheme with an improved spectral radius and a reduced likelihood of instability (e.g., $f_{j,g}$ could be the infinite-medium adjoint eigenfunction in each spatial cell). However, we have not yet encountered any physically relevant examples for which the MSED method is unstable with $f_{j,g}=1$ or for which the convergence rate is significantly improved by some choice of $f_{j,g}\neq 1$. As such, we have not found a reason to justify the additional cost of computing $f_{j,g}$. Nonetheless, this alternate grey diffusion equation should be considered if one encounters a problem in which the use of the standard grey diffusion equation results in instability.

2.3. Space-dependent Wielandt shift

The second component of the MSED method is the space-dependent Wielandt shift (SDWS) [5]. The spectral radius of the PI scheme is determined by the dominance ratio—the ratio of the second largest eigenvalue (in magnitude) to the largest eigenvalue. When problems are optically thick (e.g., realistic reactor problems), this dominance ratio approaches 1 and the PI converges slowly. In the previous section, we noted that the number of multigroup PIs required to solve Eq. (1) may be significantly reduced by leveraging the solution of the grey diffusion system. However, obtaining this grey solution still requires computational effort and, if PI is used, many iterations may be required to converge the grey diffusion system. Thus, even when the grey diffusion equation is used, a technique for reducing the dominance ratio of diffusion systems is still desired.

Before we introduce the space-dependent Wielandt shift, we first describe the standard Wielandt shift (WS). The Wielandt shift

is a well-established acceleration technique for the PI scheme which shifts the eigenvalue spectrum of a diffusion system by some estimate of the true eigenvalue, λ', in order to reduce the dominance ratio of the system [17]. The PI scheme with WS is described by the following equations:

$$-\frac{1}{\Delta x_j}\left[D_{j+\frac{1}{2},g}\frac{\phi_{j+1,g}^{(l+\frac{1}{2})}-\phi_{j,g}^{(l+\frac{1}{2})}}{\Delta x_{j+\frac{1}{2}}}-D_{j-\frac{1}{2},g}\frac{\phi_{j,g}^{(l+\frac{1}{2})}-\phi_{j-1,g}^{(l+\frac{1}{2})}}{\Delta x_{j-\frac{1}{2}}}\right]$$
$$+\sum_{t,j,g}\phi_{j,g}^{(l+\frac{1}{2})}-\sum_{g'=1}^{G}\left[\Sigma_{s0,j,g'\to g}+\lambda_j^{\prime(l)}\chi_{j,g}\nu\Sigma_{f,j,g'}\right]\phi_{j,g'}^{(l+\frac{1}{2})} \tag{9a}$$
$$=\left[\lambda^{(l)}-\lambda_j^{\prime(l)}\right]\chi_{j,g}\sum_{g'=1}^{G}\nu\Sigma_{f,j,g'}\phi_{j,g'}^{(l)},$$

$$\lambda^{(l+1)}=\frac{\sum_{g'=1}^{G}\sum_j\nu\Sigma_{f,j,g'}\left\{\lambda_j^{\prime(l)}\phi_{j,g'}^{(l+\frac{1}{2})}+\left[\lambda^{(l)}-\lambda_j^{\prime(l)}\right]\phi_{j,g'}^{(l)}\right\}}{\sum_{g'=1}^{G}\sum_j\nu\Sigma_{f,g'}\phi_{j,g'}^{(l+\frac{1}{2})}}, \tag{9b}$$

$$\phi_{j,g}^{(l+1)}=\left\|\underline{\phi}^{(l+\frac{1}{2})}\right\|^{-1}\phi_{j,g}^{(l+\frac{1}{2})}. \tag{9c}$$

Eqs. (9) and Algorithm 3 describe the Wielandt shift technique for both multigroup and grey diffusion systems. Although λ' does not have space dependence in the case of a standard Wielandt shift, we have included spatial indices on λ' so that Eqs. (9) can be used to describe both SDWS and standard WS.

Algorithm 3: A PI step accelerated by (space-dependent) Wielandt shift

Input: $\phi_{j,g}^{(l)}$, $\lambda^{(l)}$

Result: $\phi_{j,g}^{(l+1)}$, $\lambda^{(l+1)}$

1. Compute the Wielandt shift parameter $\lambda_j^{\prime(l)}$.
2. Update the scalar flux using Eq. (9a).
3. Update the eigenvalue using Eq. (9b).
4. Renormalize the scalar flux using Eq. (9c).

Typically, one determines the Wielandt shift from the most recent iterates of the eigenvalue. In the 3D multigroup diffusion code PARCS (Purdue advanced reactor core simulator) [18], the Wielandt shift is an iteration-dependent quantity that depends on the two most recent estimates of the eigenvalue:

$$\lambda_P^{\prime(l)}\equiv\max\{\lambda^{(l)}-c_1|\lambda^{(l)}-\lambda^{(l-1)}|-c_0,\lambda_{\min}\}. \tag{10}$$

Here, c_1 and c_0 are user-defined constants (with typical values of 10 and 0.02, respectively) while $\lambda_{\min}$ is chosen such that it is physically impossible for λ to be less than $\lambda_{\min}$ (typically, $\lambda_{\min}\approx 1/3$). This type of shift works well if one has a good estimate of the true eigenvalue and the eigenvalue does not change significantly from iteration to iteration (i.e., when we are near convergence).

The recently developed space-dependent Wielandt shift improves upon the PARCS shift by providing a physically-motivated shift that is more effective at the beginning of the iteration scheme, when one does not necessarily have a good estimate of the true eigenvalue [5]. Briefly, SDWS is a class of shift techniques in which the shift λ' in Eq. (9a) is allowed to vary in space. Several variants of SDWS are described by Yee et al. [5], but, in this summary, we focus on the PARCS local eigenvalue positive source (PLEPS) shift $\lambda_{PLEPS,j}^{\prime(l)}$:

$$\lambda_{PLEPS,j}^{\prime(l)}=\max\left\{\lambda_P^{\prime(l)},\min\left\{\lambda_{\infty,j},\lambda^{(l)}\right\}\right\}. \tag{11}$$

In Eq. (11), $\lambda_P^{\prime(l)}$ is the shift used in the PARCS code (Eq. (10)) and $\lambda_{\infty,j}$ is the infinite-medium eigenvalue in spatial cell j, defined by the following equation:

$$\Sigma_{t,j,g}\phi_{\infty,j,g}-\sum_{g'=1}^{G}\Sigma_{s0,j,g'\to g}\phi_{\infty,j,g'}$$
$$=\lambda_{\infty,j}\chi_{j,g}\sum_{g'=1}^{G}\nu\Sigma_{f,j,g'}\phi_{\infty,j,g'}. \tag{12}$$

Eq. (12) can be rewritten as a $G\times G$ linear system using matrix/vector notation as follows:

$$\left[\underline{\underline{\Sigma_{t,j}}}-\underline{\underline{\Sigma_{s0,j}}}\right]\underline{\phi}_{\infty,j}=\lambda_{\infty,j}\underline{\chi}_j\underline{\nu\Sigma}_{f,j}^{T}\underline{\phi}_{\infty,j}. \tag{13}$$

Here, $\underline{\underline{\Sigma_{t,j}}}$ is a $G\times G$ diagonal matrix, $\underline{\underline{\Sigma_{s0,j}}}$ is a $G\times G$ matrix, $\underline{\phi}_{\infty,j}$, $\underline{\chi}_j$, and $\underline{\nu\Sigma}_{f,j}$ are length-G column vectors, and the superscript T represents the transpose operator. The structure of the fission source allows us to deduce that there is only one non-zero eigenvalue solution to this infinite-medium problem, which can be computed directly using the following expression:

$$\lambda_{\infty,j}=\left\{\underline{\nu\Sigma}_{f,j}^{T}\left[\underline{\underline{\Sigma_{t,j}}}-\underline{\underline{\Sigma_{s0,j}}}\right]^{-1}\underline{\chi}_j\right\}^{-1}. \tag{14}$$

From Eq. (14), we see that a drawback of the PLEPS shift is that it requires the computation of $\lambda_{\infty,j}$ in each spatial cell. Each of these computations requires solving a $G\times G$ linear system. This is a trivial burden for the grey diffusion system, but not for the multigroup diffusion system.

Moreover, a drawback of both space-dependent and standard Wielandt shifts is that they can significantly increase the condition number of the diffusion system to which they are applied. There is a trade-off that must be considered when Wielandt shifts are used—although the Wielandt shift reduces the number of PIs required, it also significantly increases the number of linear solver iterations required per PI unless a *very* effective preconditioner is applied. This trade-off is beneficial for the grey diffusion system since the number of PIs required can be reduced by one to two orders of magnitude. On the multigroup system, however, the number of PIs required has already been significantly reduced from leveraging the grey diffusion system. At best, the application of a Wielandt shift on the multigroup system could save a few iterations; this would not offset the extra multigroup linear solver iterations required and the cost of computing $\lambda_{\infty,j}$. Because of this, we only apply a Wielandt shift to the grey system in MSED and leave the multigroup system unshifted.

More details regarding the advantages and disadvantages of all the variants of SDWS, as well as a detailed study on the trade-off between the dominance ratio and condition number of shifted diffusion systems, can be found in Yee et al. [5]. We note that the theory for SDWS is entirely independent of the theory for the grey diffusion system derived in the previous section. SDWS is simply a technique by which one can effectively reduce the dominance ratio of a (multigroup or grey) diffusion system. Its applications can extend beyond its use in the MSED method.

2.4. Multigrid in space

Thus far, we have not addressed an important question in the PI schemes in Algorithms 1, 2, and 3: how do we solve for $\phi^{(l+\frac{1}{2})}$ in Eqs.

(4a) and (9a), or for $\Phi^{(l,m+½)}$ in Eq. (5)? Algorithms 2 and 3 are only efficient if Eqs. (4a) and (9a) are solved in an efficient manner. For typical full-core reactor simulations, the large sizes of Eqs. (4a), (5), and (9a) prevent the use of direct linear solvers such as Gaussian elimination or LU factorization. As such, iterative solvers are needed. However, when a Wielandt shift such as the PARCS or PLEPS shift is used, Eq. (9a) is a nearly singular system whose condition number can be orders of magnitude greater than its unshifted counterpart. This can cause many standard iterative solvers such as GMRES, BiCGSTAB, or SOR, whose convergence rates depend heavily on the condition number and the diagonal dominance of the system, to converge extremely slowly or even diverge. Thus, the MSED method requires an efficient, iterative linear solver that is insensitive to the ill-conditioning caused by Wielandt shift. We have found that a multigrid (in space) linear solver fits this description.

The multigrid method is an acceleration technique for (generally simple) iterative linear solvers [3,19]. Many iterative linear solvers, often referred to as "smoothers," rapidly dampen and remove high-frequency error components, but are inefficient at reducing low-frequency error components. The multigrid method remedies this deficiency by mapping the linear system to a coarser spatial grid. When low-frequency error components are mapped onto coarser grids, their frequency is artificially increased by the coarser grid size. As a result, these error components can be more easily removed by the iterative linear solver. A "V-cycle" is generally performed, in which one repeatedly generates an error equation from the current residual, maps this error equation to a coarser grid ("restriction"), and performs linear solver iteration(s) on the error equation on the coarser grid. At the bottom of the V-cycle is generally a grid on which the system is small enough to be solved directly. Once this is done, one traverses up the V-cycle by successively interpolating errors onto finer grids until the original fine-grid is reached, and the solution on that grid updated.

Although the multigrid method has existed for decades, its use in reactor physics has been limited. Many reactor physics codes, such as MPACT, have previously used either Krylov solvers or even simpler iterative solvers such as SOR. However, the multigrid method has an extensive history as a solver or preconditioner for diffusion-like problems, especially in the field of radiative transfer [20,21]. Moreover, the diffusion equations in the MSED method can be viewed as variations of the standard Laplace problem ($\Delta u = f$), which serves as the primary example in many introductory texts for the multigrid method. Because of this, the multigrid method should be a natural and logical choice for the linear solver in MSED.

As suggested by Alcouffe [20], we choose the interpolation and restriction operators so that the leakage $D\frac{d}{dx}\phi$) is represented as a linear function when interpolated onto a finer grid. The interpolation operators for the grey diffusion system are given by:

$$\theta_{(p),2j-1} = \theta_{(p+1),j}, \tag{15a}$$

$$\theta_{(p),2j} = i^{(p),2j}_{(p+1),j}\theta_{(p+1),j} + i^{(p),2j}_{(p+1),j+1}\theta_{(p+1),j+1}, \tag{15b}$$

$$i^{(p),2j}_{(p+1),j} \equiv \left[\frac{\left\langle D_{2j+\frac{1}{2},2j+1}\right\rangle}{\Delta x_{2j+\frac{1}{2}}} + \frac{\left\langle D_{2j-\frac{1}{2},2j-1}\right\rangle}{\Delta x_{2j-\frac{1}{2}}}\right]^{-1}\frac{\left\langle D_{2j+\frac{1}{2},2j+1}\right\rangle}{\Delta x_{2j+\frac{1}{2}}}, \tag{15c}$$

$$i^{(p),2j}_{(p+1),j+1} \equiv 1 - i^{(p),2j}_{(p+1),j}. \tag{15d}$$

Here, p is an index representing the grid size—higher values of p correspond to coarser grids—and θ is a quantity being mapped between the coarse and fine grids. In matrix notation, Eqs. (15) can be written as:

$$\underline{\underline{I}}^{(p)}_{(p+1)}\underline{\theta}_{(p+1)} = \underline{\theta}_{(p)}. \tag{16}$$

In the MSED method, we define the restriction operator to be the transpose of the interpolation operator multiplied by a diagonal matrix $\underline{\underline{\mathscr{D}}}^{(p+1)}_{(p)}$:

$$\underline{\underline{I}}^{(p+1)}_{(p)}\underline{\theta}_{(p)} \equiv \underline{\underline{\mathscr{D}}}^{(p+1)}_{(p)}\left(\underline{\underline{I}}^{(p)}_{(p+1)}\right)^{T}\underline{\theta}_{(p)} = \underline{\theta}_{(p+1)}. \tag{17}$$

In this definition, $\underline{\underline{\mathscr{D}}}^{(p+1)}_{(p)}$ is used to normalize the sum of the weights in each row to 1. This restriction operator is a common choice for multigrid methods and leads to several desirable properties for the multigrid scheme [3]. With the interpolation and restriction operators defined as matrices, the coarse grid operators can be obtained using the following matrix expression:

$$\underline{\underline{M}}_{(p+1)} = \underline{\underline{I}}^{(p+1)}_{(p)}\underline{\underline{M}}_{(p)}\underline{\underline{I}}^{(p)}_{(p+1)}. \tag{18}$$

Algorithm 4: V-cycle with a red–black block Jacobi smoother for solving the fixed-source diffusion problem $\underline{\underline{M}}\underline{\phi} = \underline{g}$.

Input: $\underline{\phi}^{(q)}$

Result: $\underline{\phi}^{(q+1)}$

1. Perform one red–black block Jacobi iteration on the linear system on the original grid (p=0) to obtain $\underline{\phi}^{\left(q+\frac{1}{2}\right)}$.
2. Compute the residual on the original grid:
$$\underline{r}^{\left(q+\frac{1}{2}\right)}_{(0)} \equiv \underline{g} - \underline{\underline{M}}\,\underline{\phi}^{\left(q+\frac{1}{2}\right)}. \tag{19}$$
3. Traverse down the V-cycle. That is, for p=1,…,P−1:
   (a) Restrict the residual from grid p−1 to grid p:
   $$\underline{r}^{(q)}_{(p)} = \underline{\underline{I}}^{(p)}_{(p-1)}\underline{r}^{\left(q+\frac{1}{2}\right)}_{(p-1)}. \tag{20}$$
   (b) Perform one red–black block Jacobi iteration on the grid p error equation,
   $$\underline{\underline{M}}_{(p)}\underline{\varepsilon}_{(p)} = \underline{r}_{(p)}, \tag{21}$$
   to obtain $\underline{\varepsilon}^{\left(q+\frac{1}{2}\right)}_{(p)}$, an estimate of $\underline{\varepsilon}_{(p)}$. Here, $\underline{\varepsilon}_{(p)}$ is the coarse version of the error $\underline{\varepsilon}_{(p-1)} - \underline{\varepsilon}^{\left(q+\frac{1}{2}\right)}_{(p-1)}$.
   (c) Compute the residual of the grid p error equation:
   $$\underline{r}^{\left(q+\frac{1}{2}\right)}_{(p)} \equiv \underline{r}^{(q)}_{(p)} - \underline{\underline{M}}\,\underline{\phi}^{\left(q+\frac{1}{2}\right)}. \tag{22}$$
   We note that traversing down the V-cycle is a process by which errors of errors and residuals of error equations are computed/estimated recursively.
4. Restrict the residual from grid P−1 to the final grid, P. Solve the error equation exactly on this grid to obtain $\underline{\varepsilon}^{(q+1)}_{(p)}$.
5. Traverse up the V-cycle. That is, for p=P−1,…,1, interpolate the estimate of the error from grid p+1 to grid p, and use this result to update the error estimate on grid p and obtain $\underline{\varepsilon}^{(q+1)}_{(p)}$:
   $$\underline{\varepsilon}^{(q+1)}_{(p)} = \underline{\varepsilon}^{\left(q+\frac{1}{2}\right)}_{(p)} + \underline{\underline{I}}^{(p)}_{(p+1)}\underline{\varepsilon}^{(q+1)}_{(p+1)}. \tag{23}$$
6. Interpolate $\underline{\varepsilon}^{(q+1)}_{(1)}$ to the original grid and update $\underline{\phi}^{\left(q+\frac{1}{2}\right)}$:
   $$\underline{\phi}^{(q+1)} = \underline{\phi}^{\left(q+\frac{1}{2}\right)} + \underline{\underline{I}}^{(0)}_{(1)}\underline{\varepsilon}^{(q+1)}_{(1)}. \tag{24}$$

Algorithm 4 describes the steps in a single V-cycle in the multigrid linear solver used in MSED. For the grey system in the MSED method, multigrid is paired with a red–black Jacobi smoother. The "red–black" aspect refers to the classification of spatial cells into red and black cells in a checkerboard pattern.

Because of the checkerboard pattern and the structure of Eqs. (1) and (5), the update of the black cells only depends on the solution in the red cells, and vice versa. Thus, one can reduce the computational effort required for convergence by updating the red and black cells successively, rather than simultaneously.

For the multigroup system, we pair multigrid with a red–black block Jacobi method with blocks of size G. Despite the multigroup nature of the equations, the multigrid interpolation and restriction operators described in Eqs. (15) can still be used to transition between the spatial grids while leaving the group structure mostly intact. The quantities x and i in Eqs. (15) are group-dependent quantities in the multigroup system, but the interpolation/restriction process is still more or less the same as that of the grey system. In the multigroup case, the interpolation and restriction operators are group-dependent and treat the quantities of each group separately, while the block Jacobi smoother acts on all of the groups simultaneously to resolve the group-dependence of the flux.

This block Jacobi smoother, though simple, may not be optimal. In future work, we will study the performance of the multigrid method with other smoothers (e.g., under-relaxed Jacobi) and select the optimal smoother for the MSED method.

3. The MSED algorithm

Algorithm 5: An MSED iteration step

Input: $\phi_{j,g}^{(l)}$, $\lambda^{(l)}$

Result: $\phi_{j,g}^{(l+1)}$, $\lambda^{(l+1)}$

1. Compute the grey quantities given by Eqs. (6) using the current multigroup scalar flux $\phi_{j,g}^{(l)}$ in order to construct the grey diffusion system (Eq. (5)).
2. Perform M PIs with a space-dependent Wielandt shift on the grey diffusion equation (see Eq. (11) and Algorithm 3) to obtain the normalized grey scalar flux $\Phi_j^{(l,M)}$ and its corresponding eigenvalue $\lambda^{(l,M)}$.

Within each PI step, the grey diffusion linear system (Eq. (5) with the PLEPS shift applied and the fission source fixed) is solved using Q V-cycles. These V-cycles are described by Algorithm 4 and Q is the dynamically determined number of V-cycles required to converge the residual of the grey linear system to some specified tolerance.

3. Update the multigroup flux and eigenvalue using the grey diffusion results via Eqs. (8).
4. Consider the linear system in Eq. (4a), except with the iteration indices incremented by 1/2. Perform two V-cycles on this system to obtain $\phi_{j,g}^{(l+1)}$.

In Algorithm 5, we assemble the components described in the previous section and describe the steps required for one complete MSED iteration. We remind the reader that the steps in Algorithm 5 are illustrated in Fig. 1B. Step 2 of the MSED iteration is represented in Fig. 1B by multiple orange arrows to indicate the two layers of nested iterations (V-cycles and PIs) that are required. In Step 2, M PIs are performed on the grey diffusion system, and each PI requires some number of multigrid V-cycles to solve a fixed-source grey diffusion problem. In Step 4, the multigroup scalar flux is updated by a "partial" PI in which two multigroup V-cycles are performed on the fixed-source multigroup diffusion problem. It is "partial" in the sense that we do not fully solve this fixed-source problem, and the decision to stop at two multigroup V-cycles per MSED iteration is justified by the Fourier analysis in the next section. As noted earlier, the purpose of Step 2 is to converge the eigenvalue and the fission source, while the purpose of Step 4 is to converge the energy-dependence of the scattering source and, consequently, the multigroup scalar flux.

4. Fourier analysis

For each component of the MSED method, we performed a Fourier analysis to assess the decay rate of error modes on homogeneous problems with periodic boundary conditions. We omit the algebraically intensive derivations from our Fourier analysis and only present a summary of the relevant results.

In a homogeneous setting with periodic boundary conditions, the PLEPS shift is equivalent to setting λ' equal to the true eigenvalue, λ_∞. The Fourier analysis in this case indicates that a PI with such a shift would have a spectral radius of zero [5]. This is a rather trivial result—λ_∞ is the true eigenvalue, and it should not be a surprise that it only takes one iteration to converge the problem if we already know the eigenvalue (and are able to solve a singular linear system). In real problems, the spectral radius is not zero due to heterogeneity and/or boundary conditions. Nonetheless, as indicated by Yee et al. [5] and the results in Table 1 of Section 5, it generally only takes $O(10)$ PIs to converge when the SDWS-PLEPS shift is used.

Secondly, we performed a Fourier analysis of the multigrid V-cycle on two homogeneous, multigroup, fixed-source diffusion problems with different cross-sections. One set of cross-sections is obtained by homogenizing the UO_2 pin cell from the C5G7 problem [22], while the other set is obtained by homogenizing the center fuel pin in the Watts Bar problem [23] with the 47-group MPACT library [24]. The results of this Fourier analysis are shown in Fig. 2, where the magnitude of the decay factor $|\omega_0|$ is plotted against the spatial frequency (ξ) of the error mode. The spectral radius ρ is given by:

$$\rho = \max_{\xi} |\omega_0| \tag{25}$$

and is approximately 0.1249 and 0.1250 for the C5G7 and Watts Bar cross-sections, respectively. The two plots in Fig. 2 are nearly identical, indicating that the multigrid V-cycles are relatively insensitive to the number of groups or the cross-section values. In the grey setting, we have found through our Fourier analysis that the spectral radius is bounded by approximately 1/8, regardless of the values of the diffusion coefficient, cross-sections, grid size, and Wielandt shift. It is more difficult to properly verify this bound analytically in the multigroup Fourier analysis due to the complexity of the multigroup equations. However, we have seen in practice (i.e., in our 1D test code for simulating heterogeneous, multigroup problems) that the convergence of the multigrid V-cycle is approximately the same in both the multigroup and one-group settings for all of the problems we have considered.

Next, we performed a Fourier analysis of Algorithm 2 with the assumption that the grey and multigroup systems (in Steps 2 and 4) are solved exactly. Effectively, this analysis computes the spectral radius of an MSED iteration scheme in which the nested inner iterations (grey V-cycles, grey PIs, and multigroup V-cycles) are converged perfectly. The analysis yields the following formula for the spectral radius:

$$\rho_{MSED} = \max_{\xi} \left[\lambda_\infty \frac{\overline{\nu\Sigma}_f}{\xi^2 \overline{D}} \left(\lambda_0 \underline{\nu\Sigma}_f - \underline{\Sigma}_a \right) + \underline{\nu\Sigma}_f - \frac{\overline{\nu\Sigma}_f}{\overline{D}} \underline{D} \right]^T \left[\underline{\underline{\Sigma}}_r + \xi^2 \underline{\underline{D}} \right]^{-1} \underline{\chi}. \tag{26}$$

Here, underlined quantities are $G\times 1$ column vectors, quantities with overbars (e.g., $\overline{\nu\Sigma}_f$) are scalars obtained by dotting the corresponding column vector with the infinite-medium spectrum, ξ is the spatial frequency of the error mode, $\underline{\underline{D}}$ is a diagonal matrix whose entries are the diffusion coefficients, and $\underline{\underline{\Sigma}}_r$ is a matrix whose entry in row g and column g' is given by:

$$\Sigma_{r,g'\to g} \equiv \Sigma_{t,g}\delta_{gg'} - \Sigma_{s0,g'\to g}. \tag{27}$$

Because of the presence of the ξ^2 in the denominator of the first term of Eq. (26), it is possible for ρ to be greater than 1 as $\xi \to 0$. However, as noted earlier, we have found no realistic problems for which slow convergence or divergence is an issue. In practice, we have found that most problems (such as the 1D Watts Bar problem) converge to a tolerance of 10^{-6} in fewer than 10 MSED iterations. This agrees with the spectral radius predicted by our Fourier analysis; when we substitute either the C5G7 or Watts Bar cross-sections into Eq. (26), we obtain a spectral radius of approximately 0.1.

Lastly, we performed a Fourier analysis that allowed us to optimize the number of V-cycles performed on the multigroup diffusion system per MSED iteration. This is an important parameter since the V-cycles on the multigroup diffusion system are computationally expensive relative to the other steps in the MSED iteration scheme. In the Fourier analysis, we allowed N, the number of multigroup V-cycles per MSED iteration, to vary and computed the spectral radius for several values of N. Although Step 4 in Algorithm 5 is meant to be a PI step in which a linear system is solved, the results in Fig. 3 show that the spectral radius is nearly unchanged by increasing N beyond 2. That is, there is essentially no additional benefit from further converging the multigroup fixed-source diffusion problem in each MSED iteration by performing more than two multigroup V-cycles. The results in Fig. 3 indicate that the difference in the spectral radius for N=1 and N=2 is also small, but we have found in our numerical tests that performing at least two cycles prevents the appearance of negative multigroup scalar fluxes. Thus, we chose to use N=2 in Step 4 of Algorithm 5.

5. One-dimensional results

To test the MSED method, we have developed a test code for solving heterogeneous, multigroup diffusion eigenvalue problems in one dimension. Results from the code are shown in Table 1 for a 1D Watts Bar problem using the MPACT 47-group library. This 1D Watts Bar problem is generated from the center row of pin cells in the 2D Watts Bar problem described by Godfrey [23]. In our simulation, Δx is equal to the width of a pin cell and the cross-sections are homogenized over each pin cell. All eigenfunctions are normalized such that:

$$\left[\sum_{j=1}^{J} \Delta x_j\right]^{-1} \sum_{j=1}^{J} \sum_{g=1}^{G} \phi_{j,g} \Delta x_j = 1, \tag{28}$$

and the simulation is deemed converged when the following criteria are met:

$$\left|\lambda^{(l)} - \lambda^{(l-1)}\right| \leq 10^{-6}, \tag{29a}$$

$$\left\|\underline{\phi}^{(l)} - \underline{\phi}^{(l-1)}\right\|_2 \leq 10^{-6}. \tag{29b}$$

Here,

$$\left\|\underline{\phi}^{(l)} - \underline{\phi}^{(l-1)}\right\|_2 \equiv \sqrt{\frac{1}{JG} \sum_{j=1}^{J} \sum_{g=1}^{G} \left[\phi_{j,g}^{(l)} - \phi_{j,g}^{(l-1)}\right]^2}. \tag{30}$$

Overall, the results in Table 1 demonstrate the efficiency of the MSED method in solving 1D diffusion eigenvalue problems. More specifically, these results provide a sense of the benefit introduced by (1) leveraging the grey diffusion system in the PI scheme and (2) using a multigrid linear solver instead of other iterative linear solvers such as BiCGSTAB. By comparing cases A and D to cases F and G, we see that the grey diffusion system allows for a significant reduction in the number of multigroup inners (linear solver iterations) required. Despite the extra grey inner iterations required for convergence, we see an overall reduction in the runtime by a factor of two to three, since multigroup inners are significantly more costly than grey inners. In cases A–E and F–G, we see that the multigrid linear solver results in the lowest overall runtime. Compared to the unpreconditioned and block-Jacobi preconditioned BiCGSTAB linear solvers, using a multigrid linear solver reduces the overall runtime by a factor of two to four. The ILU-

Table 1
Results for a 1D Watts Bar problem [23] using a 1D test code and the MPACT 47G library.[a]

Method	Grey solves	Grey inners	Multigroup solves	Multigroup inners	Runtime (s)
A	69	447	7	12	7.7
B	71	6529	7	458	29.5
C	71	6076	7	224	22.4
D	72	72	7	10	10.9
E	68	72	7	17	11.1
F	–	–	17	107	21.0
G	–	–	17	54	27.5
H	69	456	7	12	7.7
I	–	–	18	112	23.0

MPACT, Michiga parallel characteristics transport.
[a] "Solves" refer to the number of times the method attempts to solve (partially or fully) the grey or multigroup system, while "inners" refer to the total number of linear solver iterations (i.e., the number of V-cycles or BiCGSTAB iterations) performed in all of the corresponding "solves." Serial runtimes are provided in the final column. A description of the methods used is provided in Table 2.

Table 2
Description of the methods used to generate the results in Table 1.

Method	Description
A	Algorithm 5 (MSED)
B	Algorithm 5 with multigrid replaced by unpreconditioned BiCGSTAB
C	Algorithm 5 with multigrid replaced by block-Jacobi preconditioned BiCGSTAB (block size G)
D	Algorithm 5 with multigrid replaced by ILU preconditioned BiCGSTAB
E	Algorithm 5 with multigrid replaced by ILU preconditioned GMRES
F	Algorithm 3 with PLEPS shift and multigrid
G	Algorithm 3 with PLEPS shift and ILU preconditioned BiCGSTAB
H	Algorithm 5 with PARCS shift and multigrid
I	Algorithm 3 with PARCS shift and multigrid

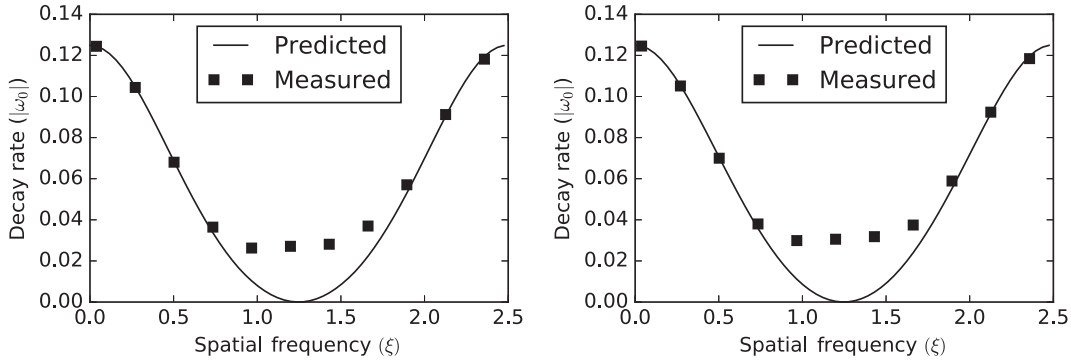

(A) C5G7 UO_2 fuel pin, $\rho = 0.1249$. (B) Watts Bar center pin, 47G MPACT lib, $\rho \approx 0.1250$.

Fig. 2. Results of our Fourier analysis of a V-cycle (Algorithm 4) for two sets of cross-sections. The solid line is the decay factor predicted by our Fourier analysis, while the square symbols represent numerical results. The disagreement in the measured and predicted values for very low decay rates is due to the numerical precision limits in the code used to verify the Fourier analysis; the toy problems converge so rapidly in these cases that it is difficult to measure the spectral radius.

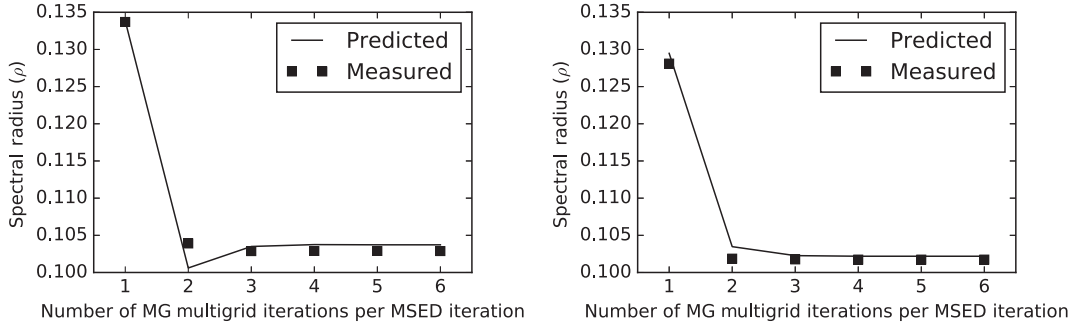

(A) C5G7 UO_2 fuel pin. (B) Watts Bar center pin, 47G MPACT lib.

Fig. 3. Spectral radius of an MSED iteration versus the number of multigroup V-cycles performed per MSED iteration. The solid line is the spectral radius predicted by the Fourier analysis, while the square symbols represent numerical results.

preconditioned Krylov methods (cases D, E, and G) produce more comparable runtimes. However, the results in Table 1 were obtained in serial and it is difficult to implement ILU preconditioners efficiently in parallel. Lastly, by comparing cases A and F to cases H and I, respectively, we see a minor improvement from using SDWS-PLEPS instead of a traditional Wielandt shift such as the PARCS shift. As noted by Yee et al. [5], the improvement provided by SDWS over traditional shifts is highly problem dependent and the improvement is not very significant in this particular problem.

The ultimate goal of our work on the MSED method is to develop a method that efficiently solves large, multigroup, 2D/3D diffusion eigenvalue problems. Although a method that is efficient in one dimension is not necessarily efficient in two or three dimensions, the results in this section serve as a proof of principle and show the potential of the MSED method. The bulk of our immediate future work will consist of implementing the MSED method as a solver for the CMFD problem in MPACT. This is not a trivial task, and many challenges will have to be overcome in order for MSED to perform as efficiently as possible in MPACT. These challenges include implementing the multigrid linear solver in parallel, finding the most efficient smoother for multigrid, and optimizing M and Q in Algorithm 5. As we implement and test the MSED method in MPACT, we will likely need to make small changes to the MSED method, and the final details of the MSED algorithm will likely differ from those presented in this paper. Future work will also include comparing MSED to other methods such as the generalized Davidson method [25], testing MSED on boiling water reactor problems and fast reactor problems, and possibly extending the MSED method to unstructured grids and/or other spatial discretizations.

6. Conclusion

We have developed and tested (in one dimension) a new MSED method for efficiently solving multigroup diffusion eigenvalue problems. The MSED method can be thought of as a PI scheme with three additional features: (1) acceleration of PI on the multigroup diffusion system via the solution of a grey diffusion system, (2) acceleration of PI via a space-dependent Wielandt shift, and (3) the use of a multigrid-in-space linear solver for the linear solves required by each PI step. Alternatively, the MSED method can be viewed as an extension of the multigrid method to nonspatial variables (see Fig. 1B) or a multilevel extension of the CMFD method (see Fig. 1A).

Results from our Fourier analysis and 1D code indicate that the MSED method can efficiently solve multigroup diffusion eigenvalue problems, as both the numerical and theoretical results indicate that the spectral radius of the MSED method is near 0.1. The 1D results indicate that the efficiency of the MSED method stems primarily from the grey diffusion system and multigrid-in-space linear solver. In these results, the grey diffusion system shifts a majority of the work from the multigroup system to the grey system, reducing the runtime by a factor of two to three when compared to algorithms in which no collapse in energy is performed. The multigrid-in-space linear solver is shown to be the most effective of the linear solvers considered, reducing the

runtime by a factor of two to four compared to block-Jacobi preconditioned BiCGSTAB and by ~20% compared to ILU-preconditioned BiCGSTAB.

Although we recognize that performance improvements in one dimension do not always translate to similar improvements in large and highly parallelized 2D/3D problems, our results to this point are promising. We are confident that, in future work, the MSED method can be efficiently implemented into MPACT as a solver for the multidimensional CMFD problem.

Conflicts of interest

All authors have no conflicts of interests to declare.

Acknowledgments

This research was supported by the Consortium for Advanced Simulation of Light Water Reactors (http://www.casl.gov), an Energy Innovation Hub (http://www.energy.gov/hubs) for Modeling and Simulation of Nuclear Reactors under US Department of Energy Contract No. DE-AC05-00OR22725. The work of the first author was also supported under a Department of Energy Nuclear Energy University Programs Graduate Fellowship.

References

[1] K.S. Smith, J.D. Rhodes III, Full-core, 2-D, LWR core calculations with CASMO-4E, in: PHYSOR 2002, October 7–10, Seoul, 2002.
[2] Mpact Team, MPACT Theory Manual Version 2.0.0," Tech. Rep. CASL-U-2015-0078-000, Consortium for Advanced Simulation of LWRs, 2015.
[3] W.L. Briggs, V.E. Henson, S.F. Mccormick, A Multigrid Tutorial, Society for Industrial and Applied Mathematics, Philadelphia, PA, 2000.
[4] B.T. Adams, J.E. Morel, A two-grid acceleration scheme for the multigroup S_N equations with neutron upscattering, Nucl. Sci. Eng. 115 (1993) 253–264.
[5] B.C. Yee, B. Kochunas, E.W. Larsen, Y. Xu, Space-dependent Wielandt shift methods for multigroup diffusion eigenvalue problems, Nucl. Sci. Eng. (2017), http://dx.doi.org/10.1080/00295639.2017.1350001.
[6] H. Finnemann, R. Boeer, R. Mueller, Y.I. Kim, Adaptive multi-level techniques for the solution of nodal transport equations, in: Proceedings of the Third European Conference on Multigrid Methods, Bonn, Germany, 2006.
[7] R. Van Geemert, Synergies of acceleration methodologies for whole-core N/TH-coupled steady-state and transient computations, in: Proceedings on the International Conference on the Physics of Reactors (PHYSOR 2006), 2006.
[8] R. Van Geemert, A multi-level surface rebalancing approach for efficient convergence acceleration of 3D full core multi-group fine grid nodal diffusion iterations, Ann. Nucl. Energy 63 (2014) 22–37.
[9] J.I. Yoon, H.G. Joo, Two-level coarse mesh finite difference formulation with multigroup source expansion nodal kernels, J. Nucl. Sci. Technol. 45 (7) (2008) 668–682.
[10] Z. Zhong, T.J. Downar, Y. Xu, M.D. Dehart, K.T. Clarno, Implementation of two-level coarse-mesh finite difference acceleration in an arbitrary geometry, two-dimensional discrete ordinates transport method, Nucl. Sci. Eng. 158 (3) (2008) 289–298.
[11] S. Schunert, Y. Wang, F. Gleicher, J. Ortensi, B. Baker, V. Laboure, C. Wang, M. Dehart, R. Martineau, A flexible nonlinear diffusion acceleration method for the S N transport equations discretized with discontinuous finite elements, J. Comput. Phys. 338 (2017) 107–136.
[12] L.R. Cornejo, D.Y. Anistratov, Nonlinear diffusion acceleration method with multigrid in energy for k-eigenvalue neutron transport problems, Nucl. Sci. Eng. 184 (2016) 4.
[13] D.Y. Anistratov, L.R. Cornejo, J.P. Jones, Stability analysis of nonlinear two-grid method for multigroup neutron diffusion problems, Journal of Computational Physics 346 (1 October 2017) 278–294.
[14] S. Balay, S. Abhyankar, M.F. Adams, J. Brown, P. Brune, K. Buschelman, L. Dalcin, V. Eijkhout, W.D. Gropp, D. Kaushik, M.G. Knepley, L.C. Mcinnes, K. Rupp, B.F. Smith, S. Zampini, H. Zhang, H. Zhang, PETSc Users Manual," Tech. Rep. ANL-95/11-Revision 3.7, Argonne National Laboratory, 2016.
[15] G. Pomraning, Grey radiative transfer, J. Quant. Spectrosc. Ra. 11 (6) (1971) 597–615.
[16] H. Park, D. Knoll, R. Rauenzahn, A. Wollaber, J. Densmore, A consistent, moment-based, multiscale solution approach for thermal radiative transfer problems, Transport. Theor. Stat. 41 (3–4) (2012) 284–303.
[17] E.L. Wachspress, Iterative Solution of Elliptic Systems, Prentice Hall, Inc., Englewood Cliffs, New Jersey, 1966.
[18] T.J. DOWNAR, et al., PARCS: purdue advanced reactor core simulator, in: PHYSOR 2002, October 7–10, Seoul, 2002.
[19] A. Brandt, Multi-level adaptive solutions to boundary-value problems, Math. Comput. 31 (138) (1977) 333–390.
[20] R.E. Alcouffe, The multigrid method for solving the two-dimensional multi-group diffusion equation, in: Advances in Reactor Computations, Proceedings of a Topical Meeting, March 28–31, Salt Lake City, 1983.
[21] R. Alcouffe, A. Brandt, J. Dendy JR., J. Painter, The multi-grid method for the diffusion equation with strongly discontinuous coefficients, SIAM J. Sci. Stat. Comp. 2 (4) (1981) 430–454.
[22] E. Lewis, M. Smith, N. Tsoulfanidis, G. Palmiotti, T. Taiwo, R. Blomquist, Benchmark specification for Deterministic 2-D/3-D MOX fuel assembly transport calculations without spatial homogenization (C5G7 MOX), NEA/NSC, 2001.
[23] A.T. Godfrey, VERA Core Physics Benchmark Progression Problem Specifications, Tech. Rep. CASL-U-2012-0131-004, Oak Ridge National Laboratory, 2014.
[24] K.S. Kim, M.L. Williams, D. Wiarda, A. Godfrey, Development of a New 47-group Library for the CASL Neutronics Simulators, 2015.
[25] R.B. Morgan, Davidson's method and preconditioning for generalized eigenvalue problems, J. Comput. Phys. 89 (1) (1990) 241–245.